Synthesis and the optical and electrochemical properties of indium(III) bis(arylimino)acenaphthene complexes

Wang, Jingyi; Ganguly, Rakesh; Yongxin, Li; Díaz, Jesus; Soo, Han Sen; García, Felipe

2017

Synthesis, optical, and electrochemical properties of indium(III) bis(arylimino)acenaphthene complexes

SCHOLARONE™
Manuscripts

Synthesis and the optical and electrochemical properties of indium(III) bis(arylimino)acenaphthene complexes

Jingyi Wang,[a] Rakesh Ganguly,[a] Li Yongxin,[a] Jesus Díaz,[b*] Han Sen Soo[a,c,d*] and Felipe García[a*]

[a.] Division of Chemistry and Biological Chemistry, School of Physical and Mathematical Sciences, Nanyang Technological University, 21 Nanyang Link 637371, Singapore.
[b.] Departamento de Química Orgánica e Inorgánica, Facultad de Veterinaria, Universidad de Extremadura, Cáceres 10071, Spain.
[c.] Singapore-Berkeley Research Initiative for Sustainable Energy (SinBeRISE), 1 Create Way, Singapore 138602.
[d.] Solar Fuels Laboratory, Nanyang Technological University, 50 Nanyang Avenue, Singapore 639798.

ABSTRACT: Aryl bis(imino)acenaphthenes (Ar-BIANs) are well-established rigid and sterically bulky diimine ligands, which are redox non-innocent and versatile π-acceptors due to their low-lying π^* orbitals, and are frequently used to bind transition metals. However, the coordination chemistry of Ar-BIAN ligands to main group elements is not as well developed as their transition metal counterparts. In particular, there are no comprehensive studies describing the spectroscopic and electrochemical properties of main group Ar-BIAN complexes. Herein, we report the synthesis and full characterization of a series of new indium(III) Ar-BIAN complexes, bearing 2,6-dialkyl (**1b** and **2b**), 4-nitro (**3b**), and 4-dimethylamino (**4b**) groups at the aryl-diimine part of the ligand. Their optical and electrochemical properties have been revealed by

UV-vis spectroscopy and cyclic voltammetry, respectively. Additionally, DFT calculations were performed to gain insights into the nature of the properties displayed.

INTRODUCTION

Redox processes and redox-active ligands play important roles in modern chemical transformations constituting exciting areas of research in coordination and organometallic chemistry,[1] and catalysis.[2] The term "*innocent ligand*" was first coined by Jørgensen as a ligand that allows the oxidation states of the central atoms to be readily determined.[3] In contrast, "*non-innocent ligands*" refer to ligands in metal complexes where the oxidation states are ambiguous and need to be experimentally determined.[1] Non-innocent ligands have energetically accessible electronic levels rendering these species redox active at mild potentials.[4] Aryl bis(imino)acenaphthenes (Ar-BIAN) belong to one class of non-innocent ligands. Ar-BIAN ligands were first reported in the 1960s and have been widely investigated as robust ligands for catalytically active transition metal centers since the early 1990s.[5] Although many coordination complexes between transition metal and Ar-BIAN ligands have been described,[6-10] their main group and lanthanide counterparts remain poorly explored, with a limited selection of main group Ar-BIAN complexes being synthesized and crystallographically characterized.[11-12]

Ar-BIAN ligands are highly tunable species that are readily synthesized from cheap and commercially available anilines and acenaphthenequinone.[13-14] Functionalized Ar-BIAN compounds are acknowledged as oxidatively and thermally stable ligands for transition metal centers. The extensive π-system of the acenaphthene ring combined with the sterically modular aniline provide a broad range of π-acceptor frameworks, offering precise control over the steric, optical, and electronic properties.[14-15] Consequently, Ar-BIAN ligands have been employed in

the preparation of numerous transition metal molecular compounds, which could be of use in

photosensitization applications due to the characterized MLCT (metal-to-ligand charge transfer)

transition from the d-orbitals of the transition metal to the π^* orbitals of the Ar-BIAN ligand.[9-10,

16] The low-lying π^* orbitals of Ar-BIAN ligands have been successfully exploited as 'capacitors'

for multi-electron reductions in redox non-innocent ligands.[17-19] Consequently, there have been

reports of transition metal Ar-BIAN complexes being used as catalysts for organic reactions such

as cycloaddition of azides and alkynes,[7-8] as well as olefin polymerization, work that had been

pioneered by M. Brookhart and coworkers using Ni(II) and Pd(II) Ar-BIAN complexes.[20-27]

More recently, Cu(II) Ar-BIAN complexes have been investigated as catalysts for the reverse

atom transfer radical polymerization (ATRP) of styrene.[28] Moreover, applications of Cu(I) Ar-

BIAN complexes as light harvesters that can absorb to the NIR region have also been reported.[6,

9, 16]

In terms of main group chemistry, however, groups 1 and 2 constitute majority of the Ar-BIAN

main group metal complexes.[17-19, 29-35] In these examples, each Ar-BIAN ligand undergoes facile

reduction due to its electron accepting nature to form the corresponding metal complex.[11] With

respect to Group 14 metals, a small number of complexes have been previously reported. For

instance, N-heterocyclic germylenes that contain anionic Ar-BIAN ligands include [(dipp-

BIAN)Ge:], [(dtb-BIAN)Ge:] (dipp = 2,6-diisopropylphenyl, dtb = 2,5-(t-Bu)$_2$Ph), and [(bph-

BIAN)Ge:] (bph = (2-PhC$_6$H$_4$)).[36] Moreover, complexes such as (dipp-BIAN)GeCl have been

prepared by reacting the neutral Ar-BIAN ligands with GeCl$_2$, where the GeCl$_2$ acts as a

reducing agent for the Ar-BIAN ligands to form their radical anionic counterparts.[37-38] On going

down this group, tin complexes supported by neutral Ar-BIAN ligands have also been described,

including [(mes-BIAN)SnCl$_4$] (mes = 2,4,6-trimethylphenyl) and [(dtb-BIAN)SnCl$_2$]).[12, 38-39] A

series of group 15 and 16 Ar-BIAN metal complexes have been previously characterized as well. For example, [(dipp-BIAN)SbCl$_3$ and [(mes-BIAN)BiCl$_3$])[12] supported by neutral Ar-BIAN ligands, and [(dipp-BIAN)E] [SnCl$_5$•THF] obtained by reduction of ECl$_3$ (E = P and As) with SnCl$_2$, followed by treatment with dipp-BIAN to give their dianionic form.[40] As for the chalcogens, the reaction of TeI$_4$ with neutral dipp-BIAN results in a two-electron reduction of the metal center to form [(dipp-BIAN)TeI$_2$], in which the ligand is neutral and the chalcogen has been reduced to the +2 oxidation state.[41] More recently, the (dipp-BIAN)SeCl$_2$ and (dipp-BIAN)SeBr$_2$ counterparts have also been described.[42] Clearly, the redox non-innocence of Ar-BIAN ligands have contributed to some rich chemistry and oxidation state ambiguity even among main group coordination compounds.

In the case of group 13 complexes, other than a limited number of boron compounds,[39, 43] only a few aluminum and gallium Ar-BIAN complexes have been isolated and structurally characterized.[43-49] In particular, until very recently,[50] there was only one crystallographically characterized example of a monometallic Ar-BIAN indium(III) complex,[12] and two reports presenting the related tetrakis(imino)py-racene (TIP) ligand.[51] Hence, the synthesis of new, heavy group 13 Ar-BIAN complexes and the evaluation of their absorption and electrochemical properties still remain under-explored areas.

Our group is interested in applying mechanochemical approach to synthetic main group compounds[52] and has recently reported the preparation of new indium(III) bis(arylimino)-acenaphthene complexes by using an essentially solvent-free mechanochemical approach.[50] The indium(III) complexes were characterized by density functional theory (DFT) calculations, electrochemistry, and UV-Vis-NIR spectroscopy. The electrochemical data suggested that the Ar-BIAN indium(III) complexes could be converted to their indium(I) congeners by mild

reducing agents, offering us the opportunity to explore the intriguing redox non-innocence of the Ar-BIAN systems. Upon reduction of the indium(III) center, these complexes show potential for applications as photosensitizers, dovetailing with our interest in the use of Earth-abundant elements in artificial photosynthesis.[16, 53-55]
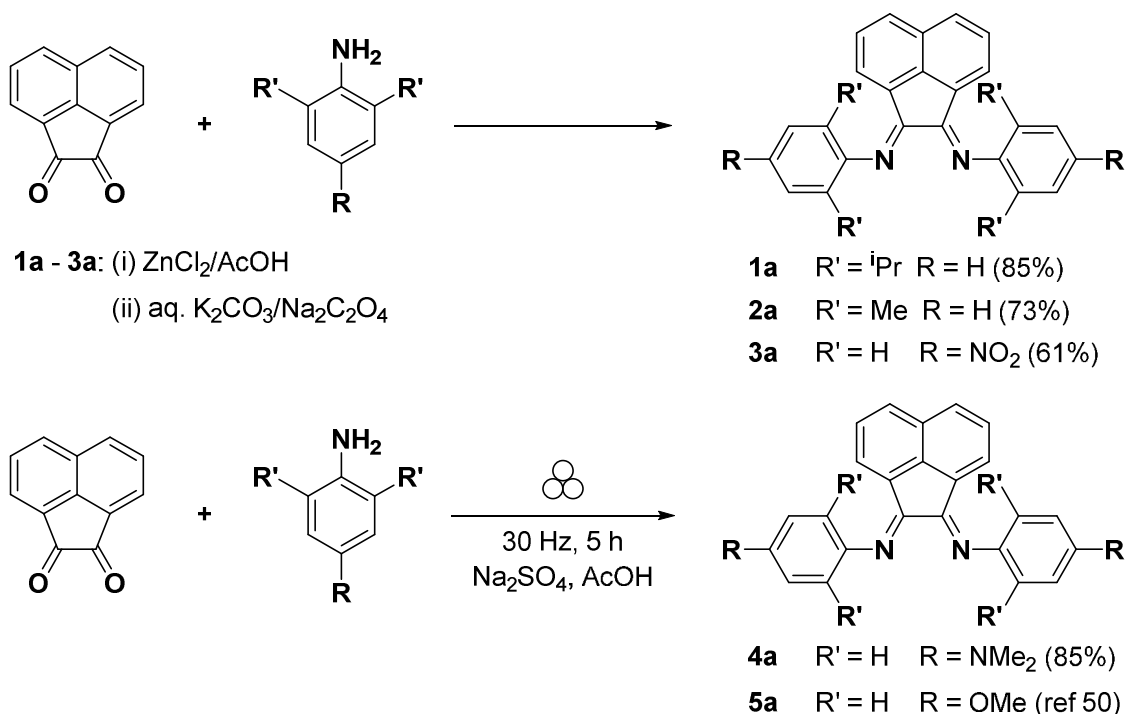
Herein, we present a family of new indium(III) Ar-BIAN complexes with the synthesis of a broad range of Ar-BIAN ligands comprising electron-donating and electron-deficient substituents on the arylimino fragment. All of the complexes reported here have been structurally characterized, and probed with electrochemical and UV-vis spectroscopic measurements, as well as DFT and TD-DFT calculations.

RESULTS AND DISCUSSION

Synthesis of complexes

The alkyl- and nitro-substituted Ar-BIAN ligands (**1a-3a**) were synthesized by condensation of acenaphthoquinone with the corresponding aniline under acidic conditions.[56-57] The Lewis acidic $ZnCl_2$ was used as the templating agent, after which de– metalation with K_2CO_3 or $Na_2C_2O_4$ was carried out (Scheme 1, top half). However, this method proved unsuccessful for the synthesis of the *para*-amino-substituted **4a**, and ligand hydrolysis was observed after the de-metalation step in an aqueous $Na_2C_2O_4$ solution. Alternatively, we have previously demonstrated that substituted Ar-BIAN ligands can be successfully synthesized *via* mechanochemical methodologies, which bypass the $ZnCl_2$ templating and subsequent de-metalation step.[50] Accordingly, **4a** was prepared via a ball-milling mechanochemical approach in the presence of a catalytic amount of acetic acid and Na_2SO_4 (Scheme 1, bottom half). The synthesis of **5a**, which

we previously reported, has been included in Scheme 1 for the completeness of our study.[50] In a typical procedure, all reactants and additives were loaded into a stainless steel grinder jar containing a 10 mm stainless steel ball (4 g weight). The reaction mixture was milled for 5 h in a Retsch MM400 mixer mill operating at 30 Hz.[58, 59] Based on the ^{1}H NMR spectra, **4a** was formed with only trace amounts of unreacted precursors. Subsequent reaction of the Ar-BIAN ligand (**1a** – **5a**) with $InCl_3$ in tetrahydrofuran (THF) afforded the respective indium(III) Ar-BIAN complexes (**1b** – **5b**). The syntheses of **1b**, **2b**, **4b**, and **5b**[60] were conducted at room temperature, whereas **3b** was prepared under reflux conditions in THF (Scheme 2).

1a - **3a**: (i) $ZnCl_2$/AcOH
(ii) aq. K_2CO_3/$Na_2C_2O_4$

1a	R' = ^{i}Pr R = H (85%)	
2a	R' = Me R = H (73%)	
3a	R' = H R = NO_2 (61%)	

30 Hz, 5 h
Na_2SO_4, AcOH

4a	R' = H R = NMe_2 (85%)	
5a	R' = H R = OMe (ref 50)	

Scheme 1 General synthetic scheme of Ar-BIAN ligands **1a** – **5a**. The symbol for mechanical milling above the arrow of the equation in the lower half has been proposed by Hanusa *et al.*[58]

InCl$_3$

THF

R.T. for **1b**, **2b**, **4b**, **5b**

Reflux for **3b**

1a	R' = ^{i}Pr	R = H
2a	R' = Me	R = H
3a	R' = H	R = NO$_2$
4a	R' = H	R = NMe$_2$
5a	R' = H	R = OMe

1b	R' = ^{i}Pr	R = H (76%)
2b	R' = Me	R = H (41%)
3b	R' = H	R = NO$_2$ (64%)
4b	R' = H	R = NMe$_2$ (68%)
5b	R' = H	R = OMe (ref 50)
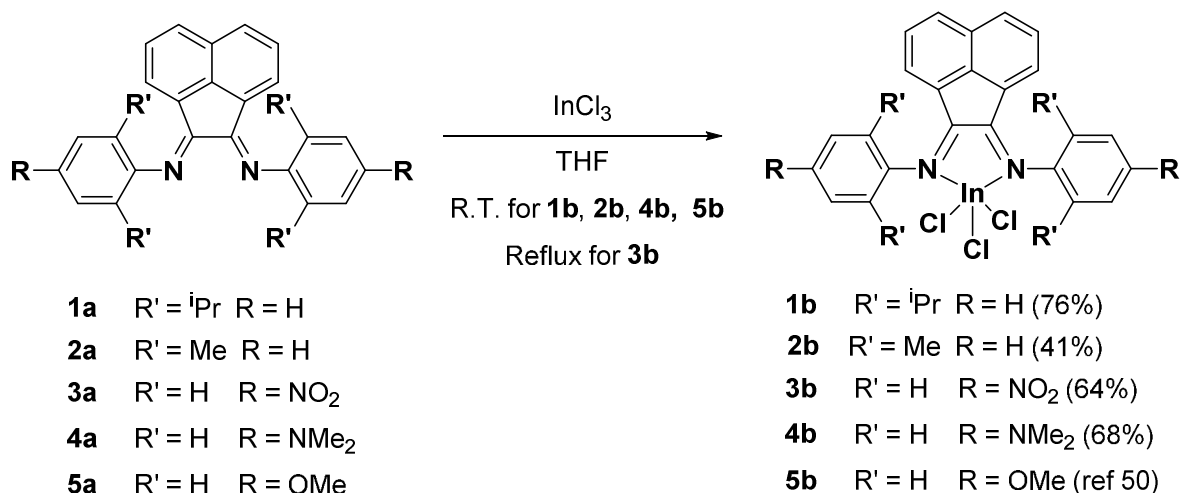
Scheme 2 Synthetic route to **1b** – **5b**.

Spectroscopic and Crystallographic Studies

The ^{1}H and ^{13}C{^{1}H} NMR spectra obtained for **1b** to **5b** concurred with the formation of coordinated, neutral Ar-BIAN ligands on indium(III). In general, the ^{1}H NMR spectra of the coordinated Ar-BIAN ligands in complexes **1b** to **5b** each exhibit a downfield shift compared to the corresponding spectra of the ligands **1a** to **5a**. Compounds **1b** and **2b** were purified by recrystallization from 1,2-dimethoxyethane (DME) and tetrahydrofuran (THF), respectively. In the case of **3b**, single crystals suitable for single crystal X-ray diffraction analysis were obtained by recrystallization from acetonitrile (ACN); however, batch purification was carried out by slow diffusion of diethyl ether (Et$_2$O) into DMF. Therefore, the characteristic DMF signals were present in the ^{1}H NMR spectrum of **3b** recorded in deuterated acetone (SI, Fig. S5). In the case of **4b** and **5b**, vapor diffusion of Et$_2$O into DMF has been used for recrystallization and, hence, one DMF molecule is coordinated to each indium(III) metal center. Thus the ^{1}H NMR spectra for both complexes reveal signals corresponding to DMF (SI, Fig. S6 and S8). All indium(III) Ar-BIAN complexes were successfully recrystallized to provide samples suitable for single crystal X-ray structural analyses (Fig. 1). We have already previously reported two structures, [(*p*-

MeOAr-BIAN)$_2$InCl$_2$]$^+$[InCl$_4$]$^-$ (**6**) and (*p*-BrAr-BIAN)InCl$_3$ (**7**), which we compare with and

refer to in this report for the completeness of our studies.[50] Compound [(*p*-MeOAr-

BIAN)$_2$InCl$_2$]$^+$[InCl$_4$]$^-$ (**6**) was originally recrystallized from ACN; however, when **6** is

recrystallized from a more strongly coordinating solvent like DMF, the mono Ar-BIAN complex

5b is formed. We attribute the formation of **5b** to the stronger coordinating ability of DMF

compared to ACN. Coordinating solvents (H$_2$O in **3b**, DMF in **4b** and **5b**) are bound to each

indium center resulting in distorted octahedral geometries for the complexes. The equatorial

bond angles range from 72.64(5)° to 101.06(2)° in **3b**, 72.85(10)° to 97.94(8)° in **4b**, and

72.68(5)° to 96.77(4)° in **5b**, deviating significantly from the ideal value of 90°. Similarly, the

axial bond angles (166.45(4)°, 164.01(7)°, and 162.18(4)° in **3b** to **5b**, respectively) also deviate

from the expected 180°. This deviation of axial and equatorial bond angles in a distorted

octahedral geometry was also reported in a similar mes-BIAN-InCl$_3$ complex.[12] In contrast, **1b**

and **2b** adopt distorted square pyramidal geometries presumably due to the increased steric

hindrance around the metal nucleus introduced by substitution of isopropyl (in **1b**) and methyl

(in **2b**) groups at the *ortho* positions of the aniline moiety. The axial bond angles range from

95.89(13)° to 110.12(6)° in **1b** and from 100.86(4)° to 107.42(19)° in **2b**, which are similar to

those in the related tetrakis(imino)pyracene (TIP) complexes that also adopt distorted square

pyramidal geometries around the indium center (94.2° – 117.4°).[51] Complex **2b** exhibits a plane

of symmetry bisecting the acenaphthene fragment and the indium metal center, making the two

diimine N and Cl atoms at the equatorial positions equivalent. The C-C and C-N bond distances

within the diimine moiety in **1b** – **5b** (ranging from 1.517(3) Å to 1.535(8) Å and from 1.274(2)

Å to 1.288(4) Å, respectively) are consistent with typical of C-C and C=N bond lengths.[12]

Therefore, complexes **1b** – **5b** can be considered to consist of neutral Ar-BIAN ligands

coordinated to indium(III) *via* dative bonds. The average In-N bond distances for **1b** and **2b** (2.341 Å and 2.320 Å, respectively) are slightly shorter than their mes-BIAN-InCl₃[12] and the dipp-TIP-InCl₃ counterparts (2.35 Å and 2.38 Å).[51] The introduction of an electron withdrawing -NO₂ group (in **3b**) and electron donating -NMe₂ (in **4b**) and -OMe groups (in **5b**) did not affect the average In-N bond distances greatly. Their average In-N bond distances (2.317 Å in **3b**, 2.324 Å in **4b**, and 2.331 Å in **5b**) remained similar to that for **1b** and **2b**. Notably, complexes **1b** to **5b** all exhibit In-Cl bond distances significantly longer than that for InCl₃(THF)₂ (2.331(3) Å).[61] The In-Cl bond distances in **1b** and **2b** range from 2.3643(17) to 2.3897(5) Å and are shorter than those in the related mes-BIAN-InCl₃, likely due to the increased electron donation from the mes-BIAN ligand in the latter, resulting in a weakening of the In-Cl bonds.[12] Although **4b** and **5b** bear ligands that are more electron-rich than **3b**, the average In-Cl bond distances in these complexes are similar (2.425 Å, 2.423 Å and 2.426 Å in **3b**, **4b**, and **5b** respectively).
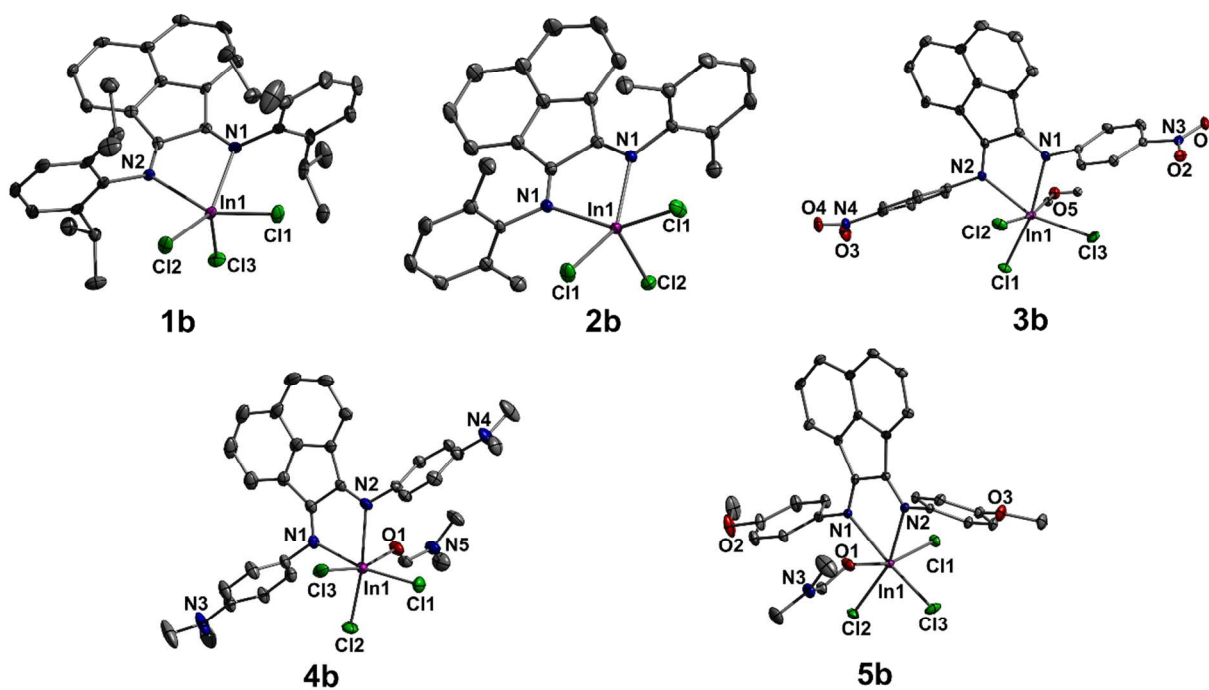

1b   **2b**   **3b**

4b   **5b**

Figure 1. Selected bond lengths (Å) and angles (°) of complexes (**1b**) In1-N1 2.342(5), In1-N2 2.339(5), In1-Cl1 2.3835(16), In1-Cl2 2.3800(17), In1-Cl3 2.3643(17); (**2b**) In1-N1 2.3196(15), In1-Cl1 2.3897(5), In1-Cl2 2.3769(7); (**3b**) In1-N1 2.3230(14), In1-N2 2.3114(14), In1-Cl1 2.4013(4), In1-Cl2 2.4722(5), In1-Cl3 2.4032(5), In1-O5 2.2733(13); (**4b**) In1-N1 2.317(3), In1-N2 2.331(3), In1-Cl1 2.4029(10), In1-Cl2 2.4241(9), In1-Cl3 2.4408(10), In1-O1 2.259(3); (**5b**) In1-N1 2.3182(14), In1-N2 2.3444(13), In1-Cl1 2.4417(4), In1-Cl2 2.4301(4), In1-Cl3 2.4058(5), In1-O1 2.2306(13). Thermal ellipsoids are drawn at the 50 % probability level. Hydrogen atoms have been omitted for clarity.

Absorption and electrochemical studies

To understand the absorption profile of the indium(III) complexes, UV-vis absorption spectroscopic measurements were carried out for **1b** − **5b**. The absorption spectra obtained for each of the complexes at 298 K are depicted in Fig. 2. Complexes **1b** to **5b** typically exhibit two major sets of absorption bands. The bands are assigned to a mixture of the intraligand π-π* charge transfer transitions between the arylimine and the acenaphthene motifs, according to the TD-DFT calculations (*vide infra*). The spectrum is significantly red-shifted when the electron donating –NMe$_2$ group is present on the di(arylimino) moiety, inducing a smaller HOMO-LUMO gap due to a more destabilized HOMO. Although inductively electron-rich alkyl groups are present in **1b** and **2b** (*i.e.*, 2,6-diisopropyl and 2,6-dimethyl), the effect is not as strong as the mesomerically donating groups in **4b** and **5b** (*i.e.*, 4-dimethylamino and 4-methoxy). This is consistent with DFT theoretical calculations from the Zysman-Colman group, where they reported that the HOMO of the ligand is destabilized by 1.1 eV when a mesomerically electron donating (-NMe$_2$) group is present within the ligand backbone, whereas a destabilization of only 0.29 eV is achieved when an inductively electron rich alkyl (2,4,6-trimethyl) group is

introduced.[14] The single intense absorption band at *ca.* 320 nm in **3b** may result from a coincidental convergence of multiple intraligand charge transfer transitions.

With an initial objective to identify a suitable reducing agent with an adequate reduction potential to obtain the indium(I) counterparts of complexes **1b** to **4b**, their redox properties were examined by cyclic voltammetry. The redox potentials of accessible reduction and oxidation waves are summarized in Table 1. The voltamogram for **5b** has not been collected in this report since its redox potential is expected to be identical to the previously reported compound **6**, which has been recorded in ACN. Since the molecular structures of **5b** and **6** are solvent dependent, their redox potentials would be affected by the solvent used.[50] All potentials are reported relative to the ferrocenium/ferrocene (Fc^+/Fc) redox couple. A direct comparison of the voltamograms of **1b** to **4b** cannot be made due to their disparate solubility properties and the differences in their coordination spheres. However, it is worth noting that the electrochemical behavior of **1b**, **2b**, and **3b** consist of four irreversible reductions and a series of oxidations (Fig. 3). The irreversibility may stem from the following. Firstly, detachment of a chloride ligand or coordination of a solvent molecule to the indium species formed during the voltammetric sweep may occur, since the reduction of the indium(III) center may involve structural changes arising from the anion dissociation. Secondly, the ligand itself may reduce due to its non-innocent nature. Thirdly, the putative indium(I) intermediates formed at the electrode surface may disproportionate, which is also supported by the experimental findings (*vide infra*). In contrast, the electrochemical behavior of **4b** in DCM showed a chemically reversible reduction wave at −1.20 V on the timescale of the experiment (Fig. 3d). The reversibility of the first reduction wave observed in **4b** suggested an increased stability of the transient $[(NMe_2Ar\text{-}BIAN)InCl_3]^-$ complex due to the stronger electron donation from **4a** to the metal center, thus, preventing

dissociation of the Ar-BIAN ligand upon reduction. This is consistent with our previous observations on the voltammogram recorded for **6** bearing electron donating -OMe groups. Compound **6** also showed an electrochemically reversible reduction wave at −1.46 V, which was attributed to the stronger electron donation from the corresponding -OMe substituted ligand to the indium(III) center.[50] Although the assignment of each reduction and oxidation processes in **1b** to **4b** was hampered by the complex processes at the electrode surface, the redox behavior of **1b** to **4b** indicate that mild reducing agents with potentials between −1.0 V to −2.0 V can be utilized to effect reduction of the In(III) complexes.[62]

In view of this, the reduction of **1b** using magnesium anthracene was attempted in THF. Interestingly, based on the ^{1}H NMR spectra and visual observations of the reaction mixture, reduction of the Ar-BIAN ligand and the indium(III) nucleus appeared to occur concurrently. Indium metal deposition was observed from the reaction mixture and the protonated reduced Ar-BIAN ligand was the only isolated reaction product as indicated by a singlet at 5.06 ppm (SI, Fig. S11). This chemical shift corresponds to the two N-H bonds of a reduced Ar-BIAN ligand, which matches the spectrum obtained from an independent reduction of ligand **1a**. Similarly, reduction reactions of **6** using $CoCp_2$ resulted in formation of the reduced Ar-BIAN ligand MeOAr-BIAN-H_2 (**8**). The presence of **8** was confirmed by ^{1}H NMR spectroscopy[63] and single crystal X-ray diffraction (SI Fig. S12). The observed formation of the reduced ligand in the attempted reduction reactions of **1b** and **6** may be attributed to the redox non-innocence of the Ar-BIAN ligands. As mentioned in the Introduction, it has been demonstrated that reduction reactions sometimes occur on the diimine ligand rather than the metal center among both main group[64-65] and transition metal complexes.[1, 66] Future studies will involve the use of: (i) bulkier aryl substituents to kinetically stabilize the indium(I) products, which has been successfully

adopted for indium(I) complexes comprising redox innocent ligands;[67] (ii) more electron-rich

aryl substituents to preclude electron transfer from the indium(I) center to the Ar-BIAN ligand;

and (iii) ligands and solvents of different electronic properties to stabilize the heteroleptic

indium(I) center. Studies involving these approaches are currently undergoing.
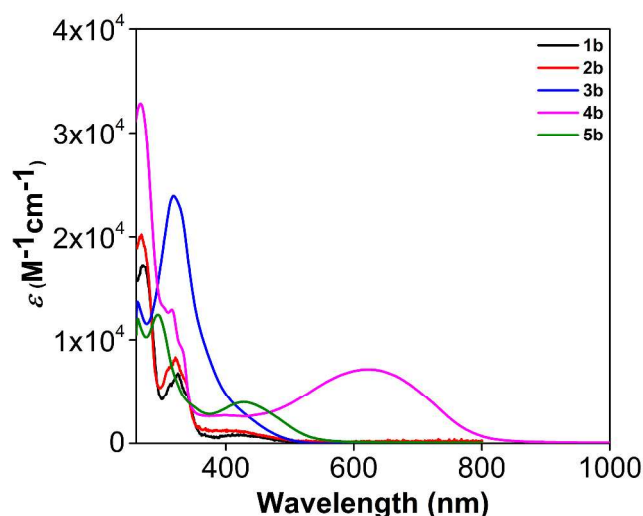

Figure 2. UV-vis spectra for **1b** and **2b** in THF, **3b** and **5b** in DMF, and **4b** in DCM solution.

All solutions were prepared, each with a concentration of 0.10 mM.

Table 1. Electrochemical data for **1b** to **4b**

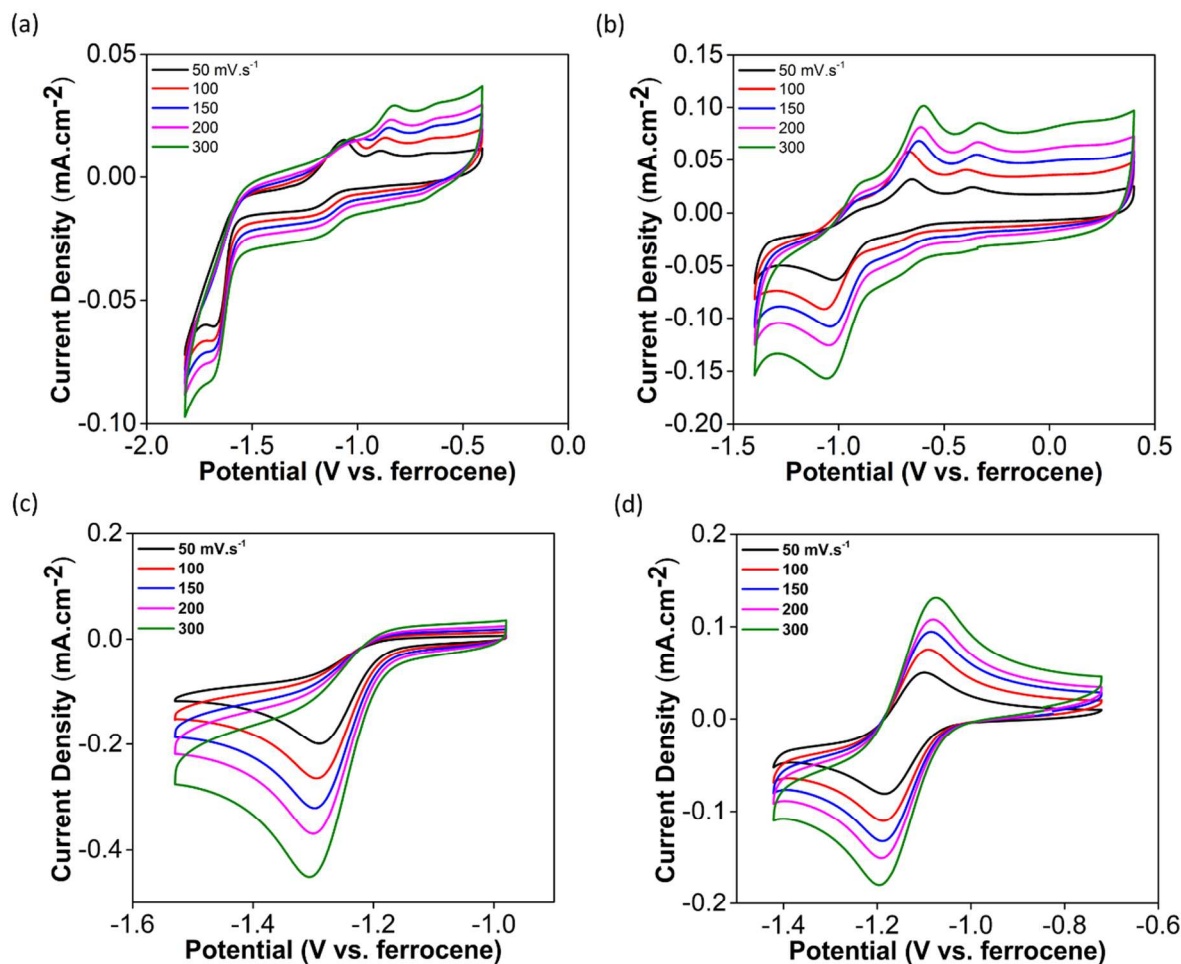|	Potential (V vs. Fc^+/Fc)	
	Cathodic peaks	Anodic peaks
1b	-1.61	-2.72
	-1.87	-2.26
	-2.41	-1.75
	-2.95	-0.54
		+0.22
2b	-1.14	-2.57
	-1.61	-2.11
	-2.30	-1.38
	-2.84	-0.98
		-0.42
3b	-1.25	-2.14
	-1.97	-1.64
	-2.32	-1.21
	-2.49	-0.08
		+0.51
4b	+0.28	-1.47
	-0.06	-1.15
	-1.24	-0.72
	-1.62	+0.44
	-1.85	+0.64

Figure 3. Cyclic voltammograms of the first reduction wave for **1b** (a) in THF, **2b** (b) in THF, **3b** (c) in DMF, and **4b** (d) in DCM solution at 298 K with 0.10 M $(nBu_4N)PF_6$ as the supporting electrolyte and glassy carbon (3 mm in diameter) as the working electrode. Data were collected using scan rates ranging from 50 to 300 $mV.s^{-1}$ and all potentials reported were referenced to Fc^+/Fc.

Computational studies

DFT and TD-DFT calculations were undertaken to predict the electronic absorption spectra of the complexes described herein. The geometry of each complex was optimized with the hybrid

functional B3LYP/6-31+G*, using the pseudo potential LANL2DZ basis set for the indium and

chlorine atoms. A larger basis set 6-31++G* was used for our previously reported complexes **6**

and **7**, with almost identical outcomes as the ones obtained from the basis set 6-31+G*. Hence,

all geometry optimizations were carried out with the smaller 6-31+G* basis set in this article

since it would be computationally cheaper. The optimized ground state structures for all

complexes agreed closely with our X-ray crystallographic studies. Each optimized structure of

1b and **2b** displays a plane of symmetry bisecting the acenaphthene and indium metal center.

The frontier orbitals illustrating the electron density distribution for **1b** to **4b** are shown in Fig. 4.

For **1b**, **2b**, and **4b**, the HOMO is mostly distributed on the di(arylimine) part of the Ar-BIAN

ligand, while the LUMO is mainly localized on the acenaphthene moiety. However, for **3b**, the

HOMO is localized on the acenaphthene bay region, whereas the LUMO has distributed

contributions throughout the entire ligand. This intriguing reversal in orbital density when

strongly electron-withdrawing groups are installed on the di(arylimine) motif is consistent with

previous DFT calculations performed on a series of Ar-BIAN ligand by Zysman-Colman and

coworkers.[14] From the TD-DFT analysis, the absorption maxima in **1b** and **2b** (λ_{max} = 320 nm)

are mainly attributed to electronic transitions from the HOMO-3 → LUMO+1, while for **3b** (λ_{max}

= 318 nm), it corresponds largely to a combination of the HOMO → LUMO+3, HOMO-1 →

LUMO+2, and HOMO-8 → LUMO transition (SI, Tables S32-S34). In the case of **4b**, the

calculated predominant contribution to the lower energy absorption maximum (λ_{max} = 630 nm)

corresponds exclusively to the HOMO→LUMO transition, whereas the higher energy UV

absorption band (λ_{max} = 267 nm) consists of a combination of contributions from HOMO-

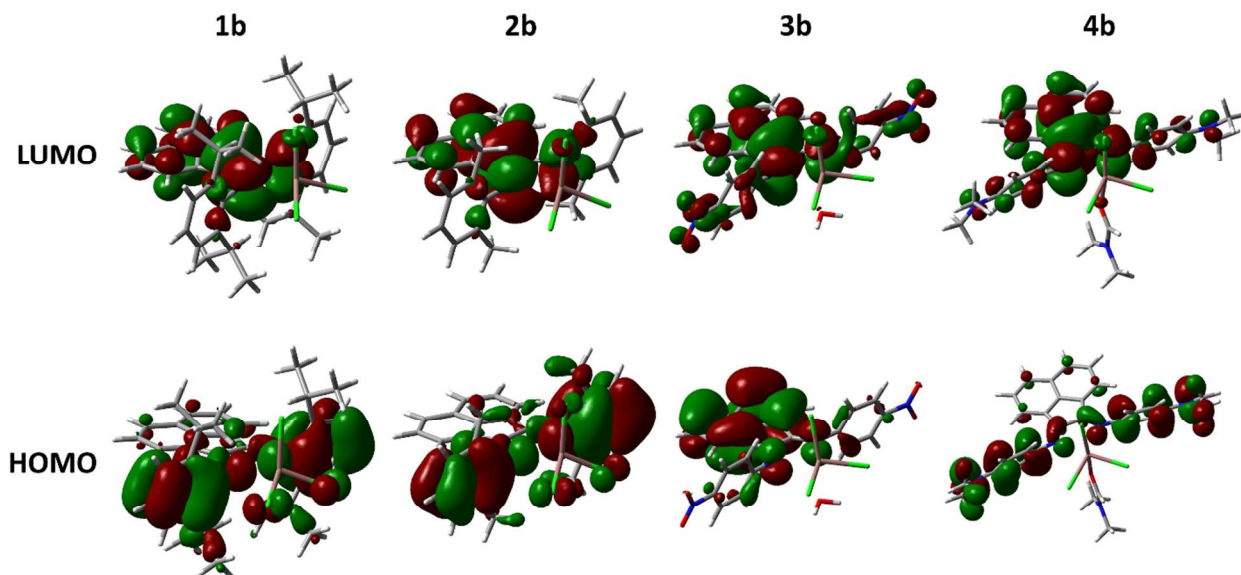14→LUMO, HOMO-15→LUMO, and HOMO→LUMO+7 transitions (SI, Table S35).

Figure 4. Electron density distributions of the frontier orbitals for **1b** to **4b**.

CONCLUSIONS

We have conducted a comprehensive investigation on the synthesis, absorption, and electrochemical properties of a series of five indium(III) complexes bearing redox non-innocent Ar-BIAN ligands. All the complexes within this study absorb light over wavelengths ranging from 380 – 800 nm, with **4b** absorbing furthest to the red region, which can be attributed to the small HOMO-LUMO gap due to the -NMe$_2$ substituent. On the other hand, the absorption spectrum of **3b** revealed a single intense band at 320 nm resulting from enlarged frontier orbital energy gaps arising from the electron withdrawing -NO$_2$ group. The CVs showed irreversible reduction waves ranging from -1.2 to -1.9 V for compounds **1b** – **3b**, whereas this reduction was observed to be chemically reversible for compound **4b** and our previously reported complex **6**. Although disproportionation and ligand reduction were observed during our attempted reduction of **1b** and **6**, we ascribe it to the non-innocent behavior of the Ar-BIAN ligand, which can accommodate the extra electrons more readily than the In metal center. Future work will involve

modifying both the steric and electronic properties of the Ar-BIAN ligands, as well as using different counter anions and ligands in heteroleptic systems to prevent electron transfer from the metal to the Ar-BIAN ligand.

EXPERIMENTAL DETAILS

General procedures

All reactions with $InCl_3$ and the recrystallization of products were performed under dry and inert atmospheres by using a combination of standard Schlenk line techniques and a Vacuum Atmospheres Company N_2 glovebox. Solvents including tetrahydrofuran (THF), diethyl ether (Et_2O), and pentane were distilled over Na/benzophenone and degassed using freeze-pump-thaw cycles prior to use. Anhydrous acetonitrile (ACN) was collected from a PURE SOLV MD-5 solvent purification system and stored in a glovebox. Anhydrous 1, 2-dimethoxyethane (DME) and dichloromethane (DCM) were distilled over calcium hydride (CaH_2) and stored in a glovebox. Anhydrous N,N-Dimethylformamide (DMF) in a Sure-Seal bottle was purchased from Sigma-Aldrich and used as received. Deuterated chloroform ($CDCl_3$) and acetonitrile (CD_3CN) were distilled over CaH_2 and stored over 4 Å molecular sieves. Deuterated acetone was distilled over potassium carbonate (K_2CO_3). All reagents were purchased from commercial sources and were used without further purification. Synthetic procedures for **6** and **7** were reported by our team previously.[50] The ^1H and $^{13}C\{^1H\}$ NMR spectra were recorded at 298 K on Bruker AV400 and BBFO 400 spectrometers. The chemical shift values are reported in parts per million (ppm) relative to TMS, using residual protonated solvents as the internal standards (^1H: $\delta = 7.26$ for $CDCl_3$ and $\delta = 1.94$ for CD_3CN; ^{13}C: $\delta = 77.2$ for $CDCl_3$, and $\delta = 118.3$ for CD_3CN). The ^{115}In NMR data have not been reported due to the large quadrupolar moments of the nuclei, which

result in broad and essentially unobservable NMR signals in the solid-state.[68-70] This is especially the case due to the low symmetry of our reported complexes.

Other Instrumentation

High-resolution mass spectra were obtained by using a Waters Q-Tof Premier, with ESI mode. Crystallographic data were recorded on a Bruker X8 CCD diffractometer. UV-vis spectroscopic measurements were performed using a Shimadzu UV-3600 UV-Vis-NIR Spectrophotometer. Cyclic voltammetry (CV) experiments were conducted in a glovebox with N_2 atmosphere, using a Biologic SP-300 potentiostat with 1.0 mM solutions of each sample and 0.10 M of tetrabutylammonium hexafluorophosphate (n-Bu$_4$NPF$_6$) as the electrolyte. Melting points were measured on an OptiMelt automated melting pointing system using sealed glass capillaries under argon and were uncorrected.

Synthesis of indium(III) complexes

(dipp-BIAN)InCl$_3$ (1b): A solution of InCl$_3$ (0.025 g, 0.11 mmol) in THF (5 mL) was added to a solution of dipp-BIAN (0.056 g, 0.11 mmol) in THF (5 mL) at room temperature. (see Supporting Information, SI, for synthesis of dipp-BIAN) The resulting orange solution was stirred overnight, after which all volatiles were removed under vacuum. The resultant orange powder was recrystallized by vapor diffusion of pentane into a DME solution of the crude product and the isolated yield was 0.061 g (76%). ^{1}H NMR (400 MHz, CDCl$_3$): δ = 0.87 (d, J = 7.2 Hz, 12 H), 1.38 (d, J = 6.8 Hz, 12 H), 3.07 (sept, J = 6.8 Hz, 4 H), 6.75 (d, J = 7.2 Hz, 2 H), 7.40 (d, J = 7.6 Hz, 4 H), 7.50-7.54 (m, 2 H), 7.60 (t, J = 8.0 Hz, 2 H), 8.17 (d, J = 8.0 Hz, 2 H). ^{13}C{^{1}H} NMR (100 MHz, CDCl$_3$): δ = 24.4, 24.8, 29.9, 125.1, 126.2, 127.8, 129.1, 129.3, 131.1, 133.2, 140.0, 140.3, 144.3, 162.7. m.p.: decomposed at 280°C HRMS (ESI+, m/z) calculated for

$C_{36}H_{40}N_2InCl_3Na$ [M+Na]$^+$ m/z = 743.1194, found 743.1179. Anal. Calcd. for $C_{36}H_{40}N_2InCl_3$: C, 59.90; H, 5.59; N, 3.88. Found: C, 59.56; H, 5.43; N, 3.82.

(2,6-Me₂Ar-BIAN)InCl₃ (2b): The procedure was identical to the one reported above for **1b**. The following quantities of reagents were used: InCl₃ (0.023 g, 0.10 mmol) in THF (5 mL), 2,6-Me₂Ar-BIAN (0.040 g, 0.10 mmol) in THF (5 mL). (see SI for synthesis of 2,6-Me₂Ar-BIAN) Orange block-like crystals suitable for single crystal X-ray analysis were obtained by recrystallization via vapor diffusion of pentane into a THF solution of the crude product and the isolated yield was 0.026 g (41%). ^{1}H NMR (400 MHz, CDCl₃): δ = 2.30 (s, 12 H), 6.79 (d, J = 7.2 Hz, 2 H), 7.28-7.30 (m, 4 H), 7.33-7.37 (m, 2 H), 7.62 (t, J = 7.8 Hz, 2 H), 8.21 (d, J = 8.4 Hz, 2 H). ^{13}C{^{1}H} NMR (100 MHz, CDCl₃): δ = 19.0, 125.8, 126.7, 128.4, 129.6 (two overlapping signals), 129.9, 131.1, 133.5, 142.1, 144.6, 162.3. m.p.: decomposed at 273°C HRMS (ESI+, m/z) calculated for $C_{28}H_{24}N_2InCl_3Na$ [M+Na]$^+$ m/z = 630.9942, found 630.9954. Anal. Calcd. for $C_{28}H_{24}N_2InCl_3 \cdot THF \cdot H_2O$: C, 54.92; H, 4.90; N, 4.00. Found: C, 55.16; H, 4.93; N, 4.26.

(p-NO₂Ar-BIAN)InCl₃ (3b): The procedure was similar to the one reported above for complex **1b** except that this reaction was carried out under reflux conditions overnight. The following quantities of compounds were used: InCl₃ (0.044 g, 0.20 mmol) and p-NO₂Ar-BIAN (0.084 g, 0.20 mmol) in THF (7 mL). (see SI for synthesis of p-NO₂Ar-BIAN) The resultant yellow solid was purified by washing with THF and the isolated yield was 0.083 g (64%). The purity of the product was confirmed by elemental analysis. Yellow block-like crystals suitable for single crystal X-ray analysis were obtained by recrystallization from an ACN solution of the crude product. ^{1}H NMR (400 MHz, acetone-d_6): δ = 7.27 (d, J = 6.8 Hz, 2 H), 7.75-7.79 (m, 6 H), 8.44 (d, J = 8.4 Hz, 2 H), 8.55-8.58 (m, 4 H). The ^{13}C{^{1}H} NMR could not be obtained due to the

poor solubility of **3b** in most of the available deuterated solvents. m.p.: decomposed after 320°C

HRMS (ESI+, *m/z*) calculated for $C_{24}H_{14}Cl_3InN_4O_4Na$ [M+Na]$^+$ *m/z* = 664.9017, found
664.9005. Anal. Calcd. for $C_{24}H_{14}Cl_3InN_4O_4 \cdot THF$: C, 46.99; H, 3.10; N, 7.83. Found: C, 46.63;
H, 3.45; N, 8.15.

(**p-NMe₂Ar-BIAN)InCl₃ (4b):** The procedure was identical to the one reported above for **1b.**
The following quantities of reagents were used: $InCl_3$ (0.066 g, 0.30 mmol) in THF (5 mL), *p*-
NMe_2Ar-BIAN (0.130 g, 0.30 mmol) in THF (5 mL). (see SI for synthesis of *p*-NMe_2Ar-BIAN)
The purple solution was stirred overnight, after which all volatiles were removed under vacuum.
The resultant deep blue solid was washed with Et_2O. Purple needle-like crystals suitable for
single crystal X-ray analysis were obtained from recrystallization by vapor diffusion of Et_2O into
a DMF solution of the crude product and the isolated yield was 0.13 g (68%). ^{1}H NMR (400
MHz, CD_2Cl_2, 25 °C, *fac*-isomer): δ = 3.09 (s, broad, 12 H), 6.88 (d, *J* = 9.2, 2 H), 7.04-7.06 (m,
4 H), 7.40 (d, *J* = 6.8, 2 H), 7.54-7.60 (m, 4 H), 8.17 (d, *J* = 8.0 Hz, 2 H) . ^{13}C{^{1}H} NMR (100
MHz, CD_2Cl_2): δ = 40.6, 40.7, 112.5, 123.0 (broad, may have peaks overlapping), 124.3, 126.1
(broad, may have peaks overlapping), 127.2, 128.8, 129.1, 131.3 (two peaks), 131.7, 132.8
(broad, may have peaks overlapping), 133.5, 143.8, 144.1, 150.9, 151.3 (broad, may have peaks
overlapping), 157.7. m.p. 198-202°C HRMS (ESI+, *m/z*) calculated for $C_{31}H_{33}N_5InCl_3Na$
[M+Na]$^+$ *m/z* = 734.0687, found 734.0652. Anal. Calcd. for $C_{31}H_{33}N_5OInCl_3 \cdot H_2O$: C, 50.95; H,
4.83; N, 9.58. Found: C, 50.90; H, 4.90; N, 9.32.

(**p-MeOAr-BIAN)InCl₃•DMF (5b):**[50] The synthetic procedure was reported in a recent
publication by our team and it has been included here for completeness. Recrystallization by
vapor diffusion of Et_2O into a DMF solution of the red solid resulted in samples suitable for
single crystal X-ray analysis. ^{1}H NMR (400 MHz, CD_3CN, *fac*-isomer): δ = 3.92 (s, 6 H), 7.16-

7.18 (m, 4 H), 7.33-7.36 (m, 4 H), 7.56-7.65 (m, 4 H), 8.31 (d, J = 6.8 Hz, 2 H). $^{13}C\{^{1}H\}$ 3.33

NMR (100 MHz, DMF-d$_7$): δ = 56.4, 114.4, 115.8, 116.0, 119.9, 120.4 (broad overlapping

peaks), 122.8, 124.3 (broad overlapping peaks), 124.6, 127.2 (broad overlapping peaks), 129.0

(broad overlapping peaks), 130.1, 130.3, 133.5, 138.7, 158.1, 160.6. HRMS (ESI+, m/z)

calculated for $C_{29}H_{27}Cl_3InN_3O_3Na$ [M+Na]$^+$ m/z = 708.0054, found 708.0081. Anal. Calcd. for

$C_{29}H_{27}N_3O_3InCl_3 \cdot H_2O$: C, 49.43; H, 4.15; N, 5.96. Found: C, 49.84; H, 4.55; N, 6.12.

Reduction of [(p-MeOAr-BIAN)$_2$InCl$_2$]$^+$[InCl$_4$]$^-$ (6): A THF solution (5 mL) of CoCp$_2$ was

added dropwise to a THF suspension (5 mL) of **6** at room temperature. The resulting brown

suspension was stirred for 2 h, after which all volatiles were removed under vacuum. The crude

purple solid was washed with Et$_2$O and the purple filtrate was filtered and concentrated. The ^{1}H

NMR experiments were conducted on the resultant purple solid. ^{1}H NMR (400 MHz, C$_6$D$_6$):

3.33 (s, 6 H), 4.93 (s, 2 H), 6.72-6.77 (m, 8 H), 7.12-7.42 (m, overlapping with signal from

C6D6), 7.43 (d, J = 8.0 Hz, 2 H).

Theoretical basis

DFT calculations were used to evaluate both the geometries and energies of the different indium

complexes possessing one or two coordinated Ar-BIAN ligands. The initial energy and geometry

optimization was carried out at the B3LYP[71-73] level with the 6-31+G* basis set for non-metal

atoms[74], together with the pseudo potential LANL2DZ[75] for the In and Cl atoms. The agreement

between the experimentally determined and the computed structures supports the method used.

Frequency calculations were carried out at this level to confirm that a minimum had been

achieved. To account for solvent effects, a reaction field calculation with radii and non-

electrostatic terms and the SMD solvation model was used.[76] All the TD-DFT calculations were carried out using the Gaussian 09 program package.[71-73, 77]

ACKNOWEDGEMENTS

ASSOCIATED CONTENT

Supporting Information. General procedures, experimental details, photophysical and electrochemical characterization protocols, ^{1}H and ^{13}C NMR spectra, crystallographic data (CCDC 1535077-1535081) and computational details. This material is available free of charge via the Internet at http://pubs.acs.org with DOI: 10.1021/acs.inorgchem.XXXXXXX.

AUTHOR INFORMATION

Corresponding Authors

* Dr. Felipe Garcia. * Dr. Han Sen Soo. *Dr. Jesus Díaz fgarcia@ntu.edu.sg, hansen@ntu.edu.sg and jdal@unex.es.

REFERENCES

1. Kim, P. B.; Elena, K. B.; Nikolai, V. Z. Metal complexes with non-innocent ligands. *Russ. Chem. Rev.* **2005**, *74,* 531.

2. Lyaskovskyy, V.; de Bruin, B. Redox Non-Innocent Ligands: Versatile New Tools to Control Catalytic Reactions. *ACS Catal.* **2012**, *2,* 270-279.

3. Jørgensen, C. K. Differences between the four halide ligands, and discussion remarks on trigonal-bipyramidal complexes, on oxidation states, and on diagonal elements of one-electron energy. *Coord. Chem. Rev.* **1966**, *1,* 164-178.

4. Chirik, P. J.; Wieghardt, K. Radical Ligands Confer Nobility on Base-Metal Catalysts. *Science* **2010**, *327,* 794-795.

5. Matei, I.; Lixandru, T. *Bul. Inst. Politeh. Iasi* **1967**, *13,* 245-255.

6. Kern, T.; Monkowius, U.; Zabel, M.; Knör, G. Mononuclear Copper(I) Complexes Containing Redox-Active 1,2-Bis(aryl-imino)acenaphthene Acceptor Ligands: Synthesis, Crystal Structures and Tuneable Electronic Properties. *Eur. J. Inorg. Chem.* **2010**, *2010,* 4148-4156.

7. Li, L.; Lopes, P. S.; Rosa, V.; Figueira, C. A.; Lemos, M. A. N. D. A.; Duarte, M. T.; Aviles, T.; Gomes, P. T. Synthesis and structural characterisation of (aryl-BIAN)copper(I) complexes and their application as catalysts for the cycloaddition of azides and alkynes. *Dalton Trans.* **2012**, *41,* 5144-5154.

8. Li, L.; Lopes, P. S.; Figueira, C. A.; Gomes, C. S. B.; Duarte, M. T.; Rosa, V.; Fliedel, C.; Avilés, T.; Gomes, P. T. Cationic and Neutral (Ar-BIAN)Copper(I) Complexes Containing Phosphane and Arsane Ancillary Ligands: Synthesis, Molecular Structure and Catalytic Behaviour in Cycloaddition Reactions of Azides and Alkynes. *Eur. J. Inorg. Chem.* **2013**, *2013,* 1404-1417.

9. Papanikolaou, P.; Akrivos, P. D.; Czapik, A.; Wicher, B.; Gdaniec, M.; Tkachenko, N. Homoleptic Bis(aryl)acenaphthenequinonediimine–CuI Complexes – Synthesis and Characterization of a Family of Compounds with Improved Light-Gathering Characteristics. *Eur. J. Inorg. Chem.* **2013**, *2013,* 2418-2431.

10. Papanikolaou, P. A.; Tkachenko, N. V. Probing the excited state dynamics of a new family of Cu(I)-complexes with an enhanced light absorption capacity: excitation-wavelength dependent population of states through branching. *Phys. Chem. Chem. Phys.* **2013**, *15,* 13128-13136.

11. Hill, N. J.; Vargas-Baca, I.; Cowley, A. H. Recent developments in the coordination chemistry of bis(imino)acenaphthene (BIAN) ligands with s- and p-block elements. *Dalton Trans.* **2009**, 240-253.

12. Hill, N. J.; Reeske, G.; Moore, J. A.; Cowley, A. H. Complexes of 1,2-bis(aryl-imino)acenaphthene (Ar-BIAN) ligands with some heavy p-block elements. *Dalton Trans.* **2006**, 4838-4844.

13. Gasperini, M.; Ragaini, F.; Gazzola, E.; Caselli, A.; Macchi, P. Synthesis of mixed Ar,Ar'-BIAN ligands (Ar,Ar'-BIAN = bis(aryl)acenaphthenequinonediimine). Measurement of the coordination strength of hemilabile ligands with respect to their symmetric counterparts. *Dalton Trans.* **2004**, 3376-3382.

14. Hasan, K.; Zysman-Colman, E. Synthesis, UV–Vis and CV properties of a structurally related series of bis(Arylimino)acenaphthenes (Ar-BIANs). *J. Phys. Org. Chem.* **2013**, *26,* 274-279.

15. El-Ayaan, U.; Paulovicova, A.; Yamada, S.; Fukuda, Y. The Crystal Structure of Bis[N-(2,6-diisopropylphenyl)imino] Acenaphthene and Studies of its Copper(I) and Copper(II) Complexes. *J. Coord. Chem.* **2003**, *56,* 373-381.

16. Kee, J. W.; Ng, Y. Y.; Kulkarni, S. A.; Muduli, S. K.; Xu, K.; Ganguly, R.; Lu, Y.; Hirao, H.; Soo, H. S. Development of bis(arylimino)acenaphthene (BIAN) copper complexes as visible light harvesters for potential photovoltaic applications. *Inorg. Chem. Front.* **2016**, *3,* 651-662.

17. Fedushkin, I. L.; Skatova, Alexandra A.; Chudakova, Valentina A.; Fukin, Georgy K.; Dechert, S.; Schumann, H. Monomeric Magnesium and Calcium Complexes Containing the Bidentate, Dianionic 1,2-Bis[(2,6-diisopropylphenyl)imino]acenaphthene Ligand. *Eur. J. Inorg. Chem.* **2003**, *2003,* 3336-3346.

18. Fedushkin, I. L.; Skatova, A. A.; Cherkasov, V. K.; Chudakova, V. A.; Dechert, S.; Hummert, M.; Schumann, H. Reduction of Benzophenone and 9(10H)-Anthracenone with the Magnesium Complex [(2,6-iPr$_2$C$_6$H$_3$-bian)Mg(thf)$_3$]. *Chem. Eur. J.* **2003**, *9,* 5778-5783.

19. Fedushkin, I. L.; Skatova, A. A.; Chudakova, V. A.; Fukin, G. K. Four-Step Reduction of dpp-bian with Sodium Metal: Crystal Structures of the Sodium Salts of the Mono-, Di-, Tri- and Tetraanions of dpp-bian. *Angew. Chem. Int. Ed.* **2003**, *42,* 3294-3298.

20. Johnson, L. K.; Killian, C. M.; Brookhart, M. New Pd(II)- and Ni(II)-Based Catalysts for Polymerization of Ethylene and .alpha.-Olefins. *J. Am. Chem. Soc.* **1995**, *117,* 6414-6415.

21. Mecking, S.; Johnson, L. K.; Wang, L.; Brookhart, M. Mechanistic Studies of the Palladium-Catalyzed Copolymerization of Ethylene and α-Olefins with Methyl Acrylate. *J. Am. Chem. Soc.* **1998**, *120,* 888-899.

22. Svejda, S. A.; Johnson, L. K.; Brookhart, M. Low-Temperature Spectroscopic Observation of Chain Growth and Migratory Insertion Barriers in (α-Diimine)Ni(II) Olefin Polymerization Catalysts. *J. Am. Chem. Soc.* **1999**, *121,* 10634-10635.

23. Tempel, D. J.; Johnson, L. K.; Huff, R. L.; White, P. S.; Brookhart, M. Mechanistic Studies of Pd(II)−α-Diimine-Catalyzed Olefin Polymerizations1. *J. Am. Chem. Soc.* **2000**, *122,* 6686-6700.

24. Ittel, S. D.; Johnson, L. K.; Brookhart, M. Late-Metal Catalysts for Ethylene Homo- and Copolymerization. *Chem. Rev.* **2000**, *100,* 1169-1204.

25. Shultz, L. H.; Brookhart, M. Measurement of the Barrier to β-Hydride Elimination in a β-Agostic Palladium−Ethyl Complex: A Model for the Energetics of Chain-Walking in (α-Diimine)PdR$^+$ Olefin Polymerization Catalysts. *Organometallics* **2001**, *20,* 3975-3982.

26. Leatherman, M. D.; Svejda, S. A.; Johnson, L. K.; Brookhart, M. Mechanistic Studies of Nickel(II) Alkyl Agostic Cations and Alkyl Ethylene Complexes: Investigations of Chain Propagation and Isomerization in (α-diimine)Ni(II)-Catalyzed Ethylene Polymerization. *J. Am. Chem. Soc.* **2003**, *125,* 3068-3081.

27. Liu, W.; Brookhart, M. Mechanistic Studies of Palladium(II)-α-Diimine-Catalyzed Polymerizations of cis- and trans-2-Butenes. *Organometallics* **2004**, *23,* 6099-6107.

28. Fliedel, C.; Rosa, V.; Santos, C. I. M.; Gonzalez, P. J.; Almeida, R. M.; Gomes, C. S. B.; Gomes, P. T.; Lemos, M. A. N. D. A.; Aullon, G.; Welter, R.; Aviles, T. Copper(II) complexes of bis(aryl-imino)acenaphthene ligands: synthesis, structure, DFT studies and evaluation in reverse ATRP of styrene. *Dalton Trans.* **2014**, *43,* 13041-13054.

29. Fedushkin, I. L.; Skatova, Alexandra A.; Chudakova, Valentina A.; Cherkasov, Vladimir K.; Fukin, Georgy K.; Lopatin, Mikhail A. Reduction of 1,2-Bis[(2,6-diisopropylphenyl)imino]acenaphthene (dpp-bian) with Alkali Metals − A Study of the

Solution Behaviour of (dpp-bian)$^{n-}$[M$^+$]$_n$ (M = Li, Na; n = 1−4) with UV/Vis, ESR and ^{1}H NMR Spectroscopy. *Eur. J. Inorg. Chem.* **2004**, *2004,* 388-393.

30. Fedushkin, I. L.; Chudakova, V. A.; Skatova, A. A.; Fukin, G. K. Solvent-free alkali and alkaline earth metal complexes of di-imine ligands. *Heteroat. Chem* **2005**, *16,* 663-670.

31. Fedushkin, I. L.; Chudakova, V. A.; Skatova, A. A.; Fukin, G. K. Solvent-free alkali and alkaline earth metal complexes of di-imine ligands. *Heteroat. Chem* **2006**, *17,* 618-618.

32. Fedushkin, I. L.; Skatova, A. A.; Chudakova, V. A.; Cherkasov, V. K.; Dechert, S.; Schumann, H. Magnesium and calcium complexes with two diimine radical-anion ligands. Molecular structure of the Ca complex with 1,2-bis[(2,6-diisopropylphenyl)imino]acenaphthene. *Russ. Chem. Bull.* **2004**, *53,* 2142-2147.

33. Fedushkin, I. L.; Khvoinova, N. M.; Skatova, A. A.; Fukin, G. K. Oxidative Addition of Phenylacetylene through C-H Bond Cleavage To Form the Mg^{II}–dpp-bian Complex: Molecular Structure of [Mg{dpp-bian(H)}(CCPh)(thf)$_2$] and Its Diphenylketone Insertion Product [Mg(dpp-bian)$^-${OC(Ph$_2$)CCPh}(thf)]. *Angew. Chem. Int. Ed.* **2003**, *42,* 5223-5226.

34. Fedushkin, I. L.; Chudakova, V. A.; Fukin, G. K.; Dechert, S.; Hummert, M.; Schumann, H. Protonation of magnesium and sodium complexes containing dianionic diimine ligands. Molecular structures of 1,2-bis{(2,6-diisopropylphenyl)imino}acenaphthene (dpp-BIAN), [(dph-BIAN)H$_2$(Et$_2$O)], and [(dpp-BIAN)HNa(Et$_2$O)]. *Russ. Chem. Bull.* **2004**, *53,* 2744-2750.

35. Fedushkin, I. L.; Skatova, A. A.; Lukoyanov, A. N.; Chudakova, V. A.; Dechert, S.; Hummert, M.; Schumann, H. Reactions of (dpp-BIAN)Mg(thf)$_3$ complex (dpp-BIAN is 1,2-bis{(2,6-diisopropylphenyl)imino}acenaphthene) with halogen-containing reagents. *Russ. Chem. Bull.* **2004**, *53,* 2751-2762.

36. Fedushkin, I. L.; Skatova, A. A.; Chudakova, V. A.; Khvoinova, N. M.; Baurin, A. Y.; Dechert, S.; Hummert, M.; Schumann, H. Stable Germylenes Derived from 1,2-Bis(arylimino)acenaphthenes. *Organometallics* **2004**, *23,* 3714-3718.

37. Fedushkin, I. L.; Khvoinova, N. M.; Baurin, A. Y.; Fukin, G. K.; Cherkasov, V. K.; Bubnov, M. P. Divalent Germanium Compound with a Radical-Anionic Ligand: Molecular Structures of (dpp-BIAN)$^{•-}$GeCl and Its Hydrochloration Products [(dpp-BIAN)(H)$_2$]$^{•+}$[GeCl3]$^-$ and [{(dpp-BIAN)(H)$_2$$^{•+}$}$_2$(Cl$^-$)]$^+$[GeCl$_3$]$^-$ (dpp-BIAN = 1,2-Bis{(2,6-diisopropylphenyl)imino}acenaphthene). *Inorg. Chem.* **2004**, *43,* 7807-7815.

38. Fedushkin, I. L.; Khvoinova, N. M.; Baurin, A. Y.; Chudakova, V. A.; Skatova, A. A.; Cherkasov, V. K.; Fukin, G. K.; Baranov, E. V. Reactions of germanium(II), tin(II), and antimony(III) chlorides with acenaphthene-1,2-diimines. *Russ. Chem. Bull.* **2006**, *55,* 74-83.

39. Hill, N. J.; Vasudevan, K.; Cowley, A. H. *Jordan J. Chem* **2006**, *1,* 47-54.

40. Reeske, G.; Hoberg, C. R.; Hill, N. J.; Cowley, A. H. Capture of Phosphorus(I) and Arsenic(I) Moieties by a 1,2-Bis(arylimino)acenaphthene (Aryl-BIAN) Ligand. A Case of Intramolecular Charge Transfer. *J. Am. Chem. Soc.* **2006**, *128,* 2800-2801.

41. Reeske, G.; Cowley, A. H. Direct reactions of tellurium tetrahalides with chelating nitrogen ligands. Trapping of TeI$_2$ by a 1,2-bis(arylimino)acenaphthene (aryl-BIAN) ligand and C-H activation of an α,α' -diiminopyridine (DIMPY) ligand. *Chem. Commun.* **2006**, 4856-4858.

42. Dutton, J. L.; Farrar, G. J.; Sgro, M. J.; Battista, T. L.; Ragogna, P. J. Lewis Base Sequestered Chalcogen Dihalides: Synthetic Sources of ChX$_2$ (Ch=Se, Te; X=Cl, Br). *Chem. Eur. J.* **2009**, *15,* 10263-10271.

43. Hilary, A. J.; Dumaresquearla, L.; Vidovic, D.; Clyburne, J. A. C. The coordination chemistry of o,o'-i-Pr$_2$C$_6$H$_3$-bis(imino)acenaphthene to group 13 trihalides. *Can. J. Chem.* **2002**, *80,* 1398-1403.

44. Schumann, H.; Hummert, M.; Lukoyanov, A. N.; Fedushkin, I. L. Monomeric Alkylaluminum Complexes (dpp-BIAN)AlR$_2$ (R = Me, Et, ^{i}Bu) Supported by the Rigid Chelating Radical-Anionic 1,2-Bis[(2,6-diisopropylphenyl)imino]acenaphthene Ligand (dpp-BIAN). *Organometallics* **2005**, *24,* 3891-3896.

45. Lukoyanov, A. N.; Fedushkin, I. L.; Hummert, M.; Schumann, H. Aluminum complexes with mono-and dianionic diimine ligands. *Russ. Chem. Bull.* **2006**, *55,* 422-428.

46. Schumann, H.; Hummert, M.; Lukoyanov, A. N.; Fedushkin, I. L. Sodium Cation Migration Above the Diimine π-System of Solvent Coordinated dpp-BIAN Sodium Aluminum Complexes (dpp-BIAN=1,2-Bis[(2,6-diisopropylphenyl)imino]acenaphthene). *Chem. Eur. J.* **2007**, *13,* 4216-4222.

47. Lukoyanov, A. N.; Fedushkin, I. L.; Schumann, H.; Hummert, M. Monoalkylaluminium Complexes Stabilized by a Rigid Dianionic Diimine Ligand: Synthesis, Solid State Structure, and Dynamic Solution Behaviour of (dpp-BIAN)AlR (R = Me, Et, ^{i}Bu). *Z. Anorg. Allg. Chem.* **2006**, *632,* 1471-1476.

48. Baker, R. J.; Jones, C.; Kloth, M.; Mills, D. P. The reactivity of gallium(I) and indium(I) halides towards bipyridines, terpyridines, imino-substituted pyridines and bis(imino)acenaphthenes. *New J. Chem.* **2004**, *28,* 207-213.

49. Fedushkin, I. L.; Lukoyanov, A. N.; Ketkov, S. Y.; Hummert, M.; Schumann, H. [(dpp-bian)Ga-Ga(dpp-bian)] and [(dpp-bian)Zn-Ga(dpp-bian)]: Synthesis, Molecular Structures, and DFT Studies of These Novel Bimetallic Molecular Compounds. *Chem. Eur. J.* **2007**, *13,* 7050-7056.

50. Wang, J.; Ganguly, R.; Yongxin, L.; Diaz, J.; Soo, H. S.; Garcia, F. A multi-step solvent-free mechanochemical route to indium(III) complexes. *Dalton Trans.* **2016**, *45,* 7941-7946.

51. Vasudevan, K. V.; Cowley, A. H. New bimetallic complexes supported by a tetrakis(imino)pyracene (TIP) ligand. *New J. Chem.* **2011**, *35,* 2043-2046.

52. Shi, Y. X.; Xu, K.; Clegg, J. K.; Ganguly, R.; Hirao, H.; Friščić, T.; García, F. The First Synthesis of the Sterically Encumbered Adamantoid Phosphazane P$_4$(N^{t}Bu)$_6$: Enabled by Mechanochemistry. *Angew. Chem. Int. Ed.* **2016**, *55,* 12736-12740.

53. Shao, H.; Muduli, S. K.; Tran, P. D.; Soo, H. S. Enhancing electrocatalytic hydrogen evolution by nickel salicylaldimine complexes with alkali metal cations in aqueous media. *Chem. Commun.* **2016**, *52,* 2948-2951.

54. Gazi, S.; Hung Ng, W. K.; Ganguly, R.; Putra Moeljadi, A. M.; Hirao, H.; Soo, H. S. Selective photocatalytic C-C bond cleavage under ambient conditions with earth abundant vanadium complexes. *Chem. Sci.* **2015**, *6,* 7130-7142.

55. Muduli, S. K.; Wang, S.; Chen, S.; Ng, C. F.; Huan, C. H. A.; Sum, T. C.; Soo, H. S. Mesoporous cerium oxide nanospheres for the visible-light driven photocatalytic degradation of dyes. *Beilstein J. Nanotechnol.* **2014**, *5,* 517-523.

56. Tu, T.; Sun, Z.; Fang, W.; Xu, M.; Zhou, Y. Robust Acenaphthoimidazolylidene Palladium Complexes: Highly Efficient Catalysts for Suzuki–Miyaura Couplings with Sterically Hindered Substrates. *Org. Lett.* **2012**, *14,* 4250-4253.

57. Gottumukkala, A. L.; Teichert, J. F.; Heijnen, D.; Eisink, N.; van Dijk, S.; Ferrer, C.; van den Hoogenband, A.; Minnaard, A. J. Pd-Diimine: A Highly Selective Catalyst System for the Base-Free Oxidative Heck Reaction. *J. Org. Chem.* **2011**, *76,* 3498-3501.

58. Rightmire, N. R.; Hanusa, T. P. Advances in organometallic synthesis with mechanochemical methods. *Dalton Trans.* **2016**, *45,* 2352-2362.

59. Garay, A. L.; Pichon, A.; James, S. L. Solvent-free synthesis of metal complexes. *Chem. Soc. Rev.* **2007**, *36,* 846-855.

60. Despite the synthesis of 5b being reported in our previous study, its structural features when crystallized in N,N-dimethylformamide (DMF) is discussed in the present paper.

61. Whittlesey, B. R.; Ittycheriah, I. P. Trichlorobis(tetrahydrofuran)indium(III). *Acta Cryst. C* **1994**, *50,* 693-695.

62. Connelly, N. G.; Geiger, W. E. Chemical Redox Agents for Organometallic Chemistry. *Chem. Rev.* **1996**, *96,* 877-910.

63. Viganò, M.; Ferretti, F.; Caselli, A.; Ragaini, F.; Rossi, M.; Mussini, P.; Macchi, P. Easy Entry into Reduced Ar-BIANH$_2$ Compounds: A New Class of Quinone/Hydroquinone-Type Redox-Active Couples with an Easily Tunable Potential. *Chem. Eur. J.* **2014**, *20,* 14451-14464.

64. Fedushkin, I. L.; Sokolov, V. G.; Piskunov, A. V.; Makarov, V. M.; Baranov, E. V.; Abakumov, G. A. Adaptive behavior of a redox-active gallium carbenoid in complexes with molybdenum. *Chem. Commun.* **2014**, *50,* 10108-10111.

65. Allan, C. J.; Cooper, B. F. T.; Cowley, H. J.; Rawson, J. M.; Macdonald, C. L. B. Non-Innocent Ligand Effects on Low-Oxidation-State Indium Complexes. *Chem. Eur. J.* **2013**, *19,* 14470-14483.

66. Klein, R. A.; Elsevier, C. J.; Hartl, F. Redox Properties of Zerovalent Palladium Complexes Containing α-Diimine and p-Quinone Ligands. *Organometallics* **1997**, *16,* 1284-1291.

67. Jurca, T.; Lummiss, J.; Burchell, T. J.; Gorelsky, S. I.; Richeson, D. S. Capturing In$^+$ Monomers in a Neutral Weakly Coordinating Environment. *J. Am. Chem. Soc.* **2009**, *131,* 4608-4609.

68. Chen, F.; Ma, G.; Cavell, R. G.; Terskikh, V. V.; Wasylishen, R. E. Solid-state ^{115}In NMR study of indium coordination complexes. *Chem. Commun.* **2008**, 5933-5935.

69. Hamaed, H.; Johnston, K. E.; Cooper, B. F. T.; Terskikh, V. V.; Ye, E.; Macdonald, C. L. B.; Arnold, D. C.; Schurko, R. W. A 115In solid-state NMR study of low oxidation-state indium complexes. *Chem. Sci.* **2014**, *5,* 982-995.

70. Chen, F.; Ma, G.; Bernard, G. M.; Cavell, R. G.; McDonald, R.; Ferguson, M. J.; Wasylishen, R. E. Solid-State 115In and 31P NMR Studies of Triarylphosphine Indium Trihalide Adducts. *J. Am. Chem. Soc.* **2010**, *132,* 5479-5493.

71. Becke, A. D. Density-functional exchange-energy approximation with correct asymptotic behavior. *Phys. Rev. A* **1988**, *38,* 3098-3100.

72. Lee, C.; Yang, W.; Parr, R. G. Development of the Colle-Salvetti correlation-energy formula into a functional of the electron density. *Phys. Rev. B* **1988**, *37,* 785-789.

73. Becke, A. D. Density‐functional thermochemistry. III. The role of exact exchange. *J. Chem. Phys.* **1993**, *98,* 5648-5652.

74. Hehre, W. J.; Radom, L.; Pople, J. A.; Schleyer, P. V. R., *Ab Initio Molecular Orbital Theory.* Wiley: New York, 1986.

75. Hay, P. J.; Wadt, W. R. Ab initio effective core potentials for molecular calculations. Potentials for the transition metal atoms Sc to Hg. *J. Chem. Phys.* **1985**, *82,* 270-283.

76. Marenich, A. V.; Cramer, C. J.; Truhlar, D. G. Universal Solvation Model Based on Solute Electron Density and on a Continuum Model of the Solvent Defined by the Bulk Dielectric Constant and Atomic Surface Tensions. *J. Phys. Chem. B* **2009**, *113,* 6378-6396.

77.   Frisch, M. J.; Trucks, G. W.; Schlegel, H. B.; Scuseria, G. E.; Robb, M. A.; Cheeseman, J.
      R.; Scalmani, G.; Barone, V.; Mennucci, B.; Petersson, G. A.; Nakatsuji, H.; Caricato, M.;
      Li, X.; Hratchian, H. P.; Izmaylov, A. F.; Bloino, J.; Zheng, G.; Sonnenberg, J. L.; Hada,
      M.; Ehara, M.; Toyota, K.; Fukuda, R.; Hasegawa, J.; Ishida, M.; Nakajima, T.; Honda, Y.;
      Kitao, O.; Nakai, H.; Vreven, T.; Montgomery Jr., J. A.; Peralta, J. E.; Ogliaro, F.;
      Bearpark, M. J.; Heyd, J.; Brothers, E. N.; Kudin, K. N.; Staroverov, V. N.; Kobayashi, R.;
      Normand, J.; Raghavachari, K.; Rendell, A. P.; Burant, J. C.; Iyengar, S. S.; Tomasi, J.;
      Cossi, M.; Rega, N.; Millam, N. J.; Klene, M.; Knox, J. E.; Cross, J. B.; Bakken, V.;
      Adamo, C.; Jaramillo, J.; Gomperts, R.; Stratmann, R. E.; Yazyev, O.; Austin, A. J.;
      Cammi, R.; Pomelli, C.; Ochterski, J. W.; Martin, R. L.; Morokuma, K.; Zakrzewski, V.
      G.; Voth, G. A.; Salvador, P.; Dannenberg, J. J.; Dapprich, S.; Daniels, A. D.; Farkas, Ö.;
      Foresman, J. B.; Ortiz, J. V.; Cioslowski, J.; Fox, D. J. *Gaussian 09*, Gaussian, Inc.:
      Wallingford, CT, USA, 2009.

1
2
3
4
5
6
7
8
9
10
11
12
13
14
15
16
17
18
19
20
21
22
23
24
25
26
27
28
29
30
31
32
33
34
35
36
37
38
39
40
41
42
43
44
45
46
47
48
49
50
51
52
53
54
55
56
57
58
59
60

TOC graphic "For Table of Contents Only"

The synthesis and spectroscopic studies of four new indium(III) Ar-BIAN complexes, bearing 2,6-dialkyl (**1b** and **2b**), 4-nitro (**3b**), and 4-dimethylamino groups (**4b**) at the aryl-diimine part of the ligand are reported and DFT calculations have been performed to gain insights into the nature of the optical properties displayed.
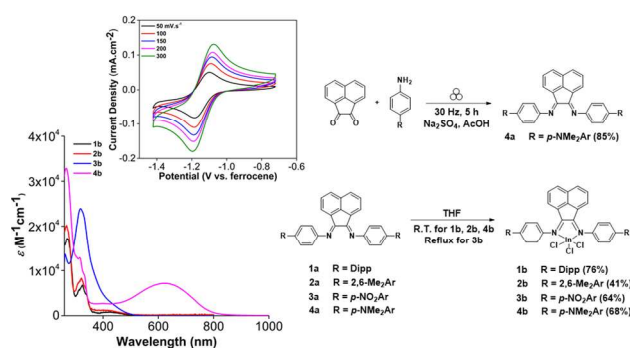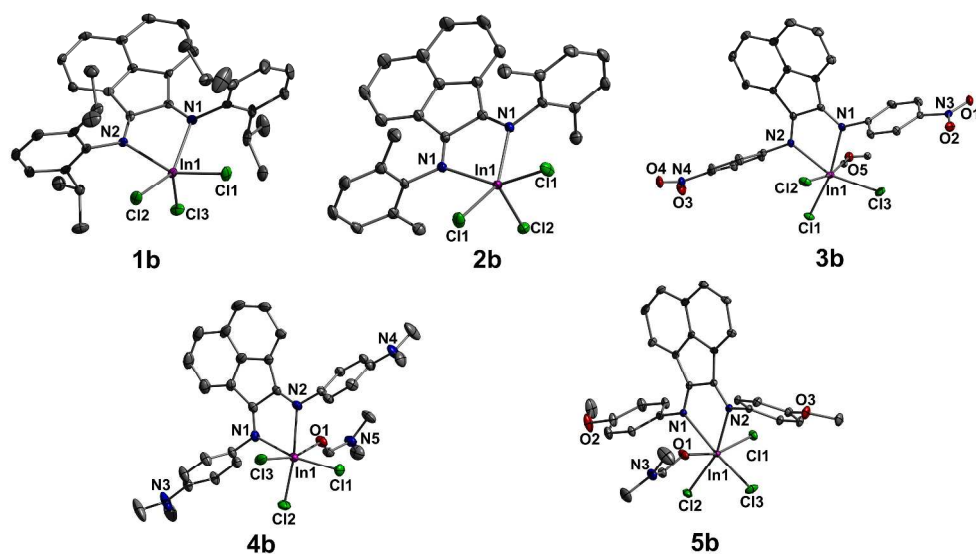
Figure 1. Selected bond lengths (Å) and angles (°) of complexes (1b) In1-N1 2.342(5), In1-N2 2.339(5), In1-Cl1 2.3835(16), In1-Cl2 2.3800(17), In1-Cl3 2.3643(17); (2b) In1-N1 2.3196(15), In1-Cl1 2.3897(5), In1-Cl2 2.3769(7); (3b) In1-N1 2.3230(14), In1-N2 2.3114(14), In1-Cl1 2.4013(4), In1-Cl2 2.4722(5), In1-Cl3 2.4032(5), In1-O5 2.2733(13); (4b) In1-N1 2.317(3), In1-N2 2.331(3), In1-Cl1 2.4029(10), In1-Cl2 2.4241(9), In1-Cl3 2.4408(10), In1-O1 2.259(3); (5b) In1-N1 2.3182(14), In1-N2 2.3444(13), In1-Cl1 2.4417(4), In1-Cl2 2.4301(4), In1-Cl3 2.4058(5), In1-O1 2.2306(13). Thermal ellipsoids are drawn at the 50 % probability level. Hydrogen atoms have been omitted for clarity.
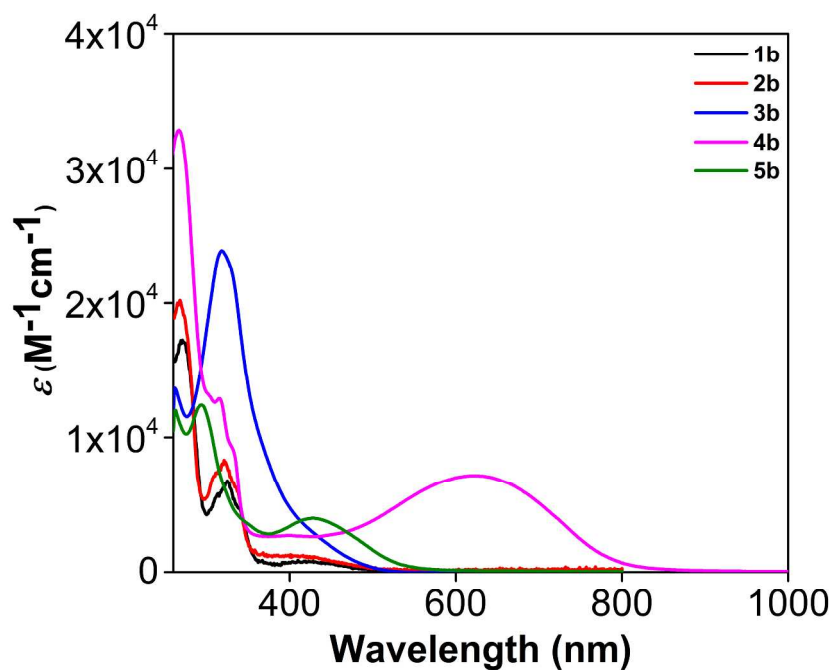
451x254mm (300 x 300 DPI)

Figure 2. UV-vis spectra for 1b and 2b in THF, 3b and 5b in DMF, and 4b in DCM solution. All solutions were prepared, each with a concentration of 0.10 mM.
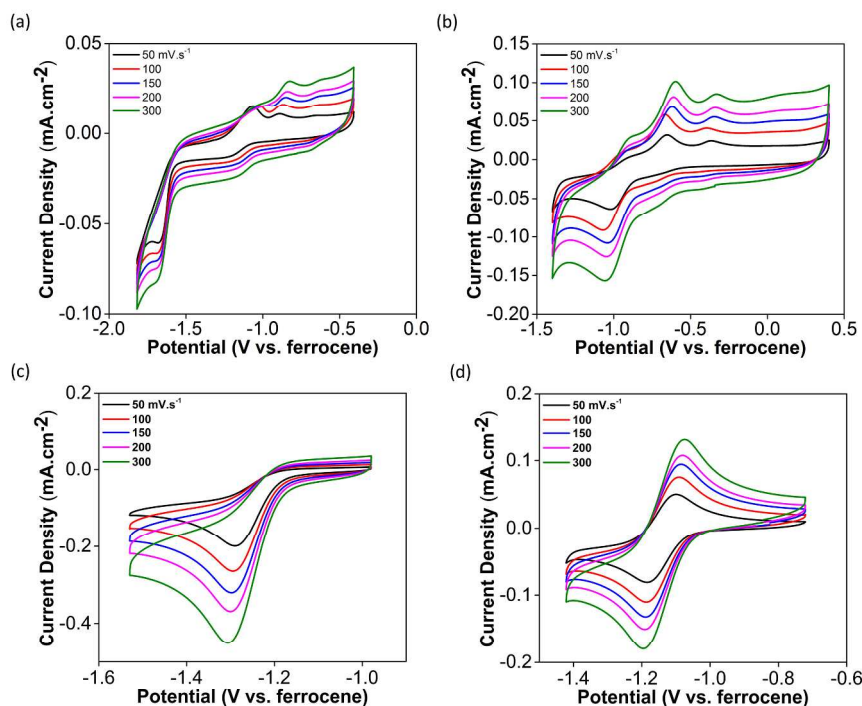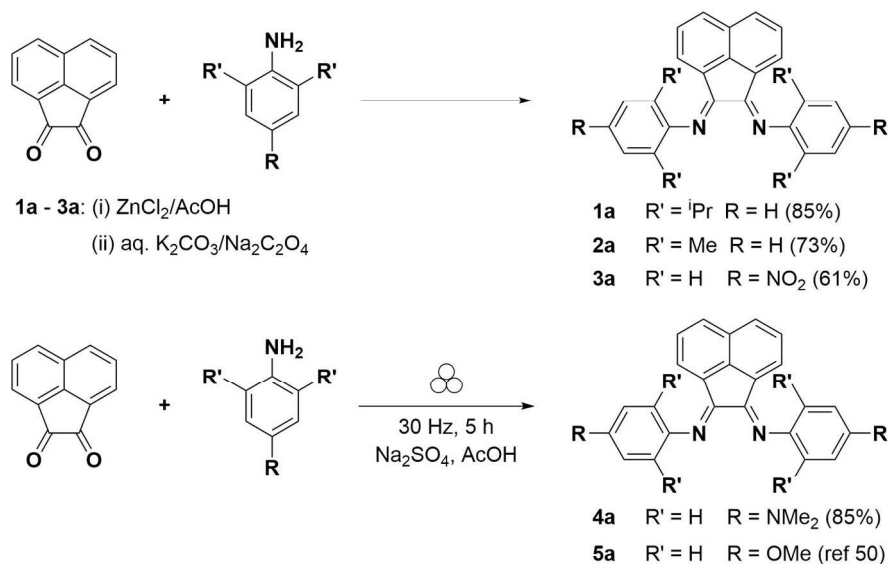
254x190mm (300 x 300 DPI)

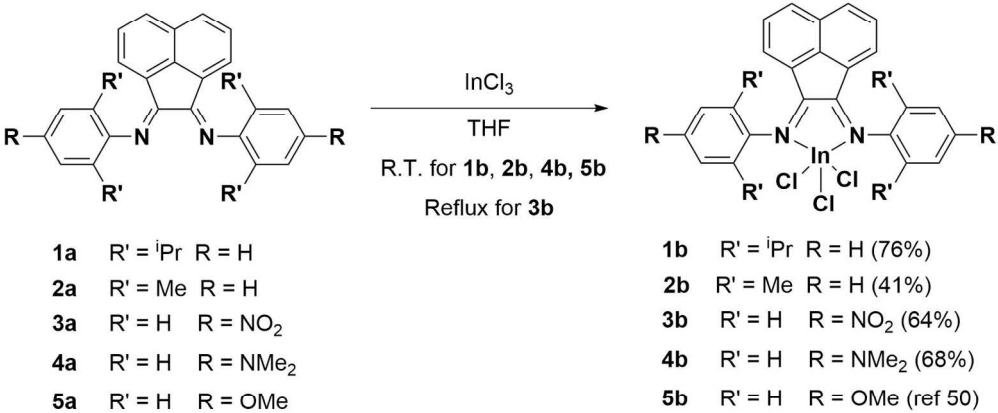Figure 3. Cyclic voltammograms of the first reduction wave for 1b (a) in THF, 2b (b) in THF, 3b (c) in DMF, and 4b (d) in DCM solution at 298 K with 0.10 M (nBu4N)PF6 as the supporting electrolyte and glassy carbon (3 mm in diameter) as the working electrode. Data were collected using scan rates ranging from 50 to 300 mV.s-1 and all potentials reported were referenced to Fc+/Fc.

254x190mm (300 x 300 DPI)

Scheme 1 General synthetic scheme of Ar-BIAN ligands 1a – 5a. The symbol for mechanical milling above the arrow of the equation in the lower half has been proposed by Hanusa et al.58

338x190mm (300 x 300 DPI)

1
2
3
4
5
6
7
8
9
10
11
12
13
14
15
16
17
18
19
20
21
22
23
24
25
26
27
28
29
30
31
32
33
34
35
36
37
38
39
40
41
42
43
44
45
46
47
48
49
50
51
52
53
54
55
56
57
58
59
60

1a	R' = ^{i}Pr	R = H
2a	R' = Me	R = H
3a	R' = H	R = NO$_2$
4a	R' = H	R = NMe$_2$
5a	R' = H	R = OMe

InCl$_3$

THF

R.T. for **1b**, **2b**, **4b**, **5b**

Reflux for **3b**

1b	R' = ^{i}Pr	R = H (76%)
2b	R' = Me	R = H (41%)
3b	R' = H	R = NO$_2$ (64%)
4b	R' = H	R = NMe$_2$ (68%)
5b	R' = H	R = OMe (ref 50)

Scheme 2 Synthetic route to 1b – 5b.

338x190mm (300 x 300 DPI)